

---

---

PHYSICS OF SOLID STATE  
AND CONDENSED MATTER

---

---

## Simulation of Graphite Oxidation in Oxygen at 400–800°C

A. N. Odeichuk and A. I. Komir

*Renewable Energy Sources and Sustainable Technologies, Science and Production Establishment of the Kharkov Institute of Physics and Technology, National Science Center, Kharkov, 61108 Ukraine*

*e-mail: anodeychuk@kipt.kharkov.ua*

**Abstract**—A computer model of nuclear-grade graphite is proposed that allows a simulation of graphite-sample oxidation to be performed (with an error 7%) taking into account the granulometric composition, porosity, and density. The results from simulating the GMZ graphite oxidation in the regime of chemical kinetics showed a satisfactory agreement with experimental data.

**Keywords:** computer simulation, oxidation of graphite, structural materials, nuclear power systems, granulometric composition

**DOI:** 10.1134/S1547477115020181

### ANALYSIS OF MODELS OF CARBON-MATERIAL OXIDATION

Active works have been underway on creating Generation IV nuclear power systems, which makes it necessary to investigate reactor-core components and, in particular, study the properties and behavior of nuclear-grade graphite in oxidative environments at high temperatures. A large amount of experimental works on studying regularities of the process of carbon-material oxidation has been carried out [1, 3, 4, 8, 9], which makes it possible to get an idea of the main phases of the oxidation process and also to perform the appropriate physical and mathematical description; however, insufficient attention is paid to studies of simulating these processes: the influence of granulometric composition and porosity of graphite is not taken into account.

Therefore, in [1], the oxidation of IG-110 graphite under different conditions was considered. The experiments were carried out with the following parameters: temperature ranges of 540–600°C and 700–1500°C, ingress rates of 3–18 L/min and 40 L/min, and oxygen concentrations of 2.5–32% and 2.5–20% with an area accessible for a reaction of 19.792 mm<sup>2</sup>. The work was based on the Arrhenius equation for which the coefficients ( $n = 0.75 \pm 0.146$ ) and the activation energy value ( $E_a = 218 \pm 4$  kJ/mol) were refined. The proposed model is asserted to encompass the parameters corresponding to the parameter range of high-temperature gas-cooled reactors.

The oxidation process was simulated in the cylindrical coordinate system. During simulation, the following parameters of the graphite sample were calculated: temperature, density, and heat capacity. Blowing around the sample was conducted bottom-up in parallel to its side surface. The paper also presents dis-

tributions of O<sub>2</sub>, CO, and CO<sub>2</sub> in the environment. However, the paper ignored the porosity and granulometric composition of the sample and also a variation in the cell volume with an increase in the sample radius, which might lead to an error in simulation of its oxidation. Estimating the error seems impossible because accuracy of calculations depending on the cell dimensions is not indicated in the work.

In [2], the following stages of graphite oxidation are analyzed:

- (a) transport of oxidant to the graphite surface;
- (b) adsorption of oxidant onto the graphite surface (physical adsorption);
- (c) formation of carbon–oxide bonds (chemisorption);
- (d) formation of carbon–hydroxide bonds (for reactions with water);
- (e) breaking of carbon–carbon bonds;
- (f) desorption of carbon monoxide or another reaction product;
- (g) transport of reaction products from the surface.

From the stages listed above, it follows that the factors influencing the rate of oxidation reaction are

- (a) intensity of the oxidant supply to the surface;
- (b) partial pressure of the oxidant;
- (c) the reaction zone is accessible for the oxidant on the surface;
- (d) amount and distribution of catalytic impurities in graphite;
- (e) temperature;
- (f) intensity of removal of reaction products;
- (g) damages to graphite inflicted by fast neutrons;

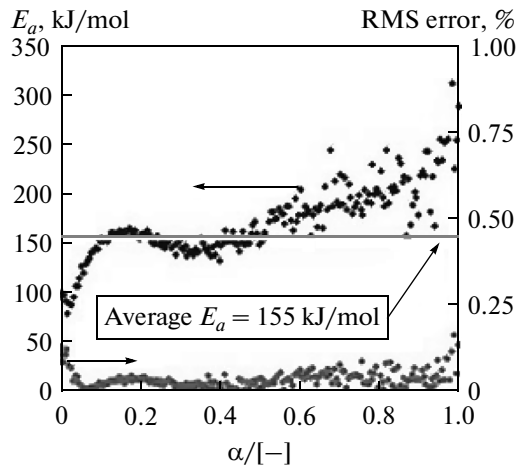


Fig. 1. Dependence of activation energy on sample mass reduction.

(h) amount of the substance preliminarily oxidized (radiolytically or by annealing);

(i) coefficient of effective diffusion.

It is noted that oxidation almost does not occur at temperatures less than 350°C. With temperature growth, beginning from 400°C, the oxidation becomes measurable. The water as an oxidant increases the threshold of oxidation reaction up to 800°C.

In [3], Mohamed S. El- Genk et al. investigated properties of IG-110, IG-430, and NBG-25 graphite. The rate of oxidant diffusion deep into graphite vs. temperature is also considered, and it is offered to divide the oxidation into three regimes:

(1) a regime that is restricted to the diffusion in the boundary layer (in this regime, the oxidant concentration decreases linearly in the thin boundary layer);

(2) diffusive regime, the diffusion is restricted to diffusion inside pores (in this regime, the oxidant is inside the sample volume and its concentration nonlinearly drops to zero at the certain depth of the sample);

(3) regime that is restricted to chemical kinetics (in this regime, the oxidant fills the entire volume of the sample with a certain concentration reducing into the depth nonlinearly and insignificantly).

Presented as plots, the experimental and theoretical dependences of mass loss on the oxidation time for IG-110 graphite are analyzed; their quantitative estimation shows that a mean absolute error is 21%. The distributions of energy of the oxidant adsorption and desorption, as well as the sample gasification rates, are also discussed in the work.

However, Mohamed S. El-Genk et al. in [3], as well as the authors of [1], did not take into account a granulometric composition of the sample, which may substantially influence the simulation of the oxidation process.

In [4], the refined coefficients of the Arrhenius equation are given for isothermal conditions at temperatures of 600, 612, and 625°C and with a rate of temperature growth of 1, 2, and 10°C/min. The dependence of activation energy on the sample depletion and its rms error are analyzed (Fig. 1). The average activation energy is shown to be 155 kJ/mol.

The proposed analytical description of the oxidation process poorly describes the experimental data.

It should be also noted that, in the literature, analytical models are described, e.g., in [5–7], in which the polynomial approximation of experimental data is used. However, this approach does not take into account the physical nature of oxidation, which yields substantial errors in calculations when going beyond the range of approximated values.

In [8, 9], data on the effective diffusion of oxygen and water to graphite are given, and the graphite density deep into the sample is analyzed after oxidation for 5 h in air at a temperature of 973 K. The models developed in [8, 9] assume that the simulation is performed with the diffusion averaged over the sample, which does not allow the graphite inhomogeneity to be taken into account.

In most existing models, the division into the oxidation regimes mentioned above is used where the oxidant diffusion deep into the sample is one model parameter; thus, porosity needs to be taken into consideration while the numerical simulation is conducted. The construction of a model without this characteristic substantially reduces the reaction surface of graphite in oxidation within a temperature range up to 1200°C.

In [10], the impact of grind on the oxidation rate is also investigated and it is said that the rate increases in the case of mechanical action on natural graphite. Consequently, when the oxidation model is under development, a granulometric composition of the graphite structure should be taken into account.

Thus, the development of a simulation model of oxidation of nuclear-grade graphite at high temperatures which takes into account its porosity and granulometric composition, the diffusive penetration of the oxidant, temperature, and linear dimensions is rather urgent. Accounting for these factors will enable the oxidation of carbon components to be simulated under operating conditions of Generation IV nuclear power systems, the working temperatures of which are plotted in Fig. 2 [11].

## SIMULATION MODEL

The simulation model is based on partitioning the sample into multiple cubic unit cells (Fig. 3). A unit cell is characterized by mass and linear dimensions. A graphite sample is described using three-dimensional matrix  $V_{\Delta x \times \Delta y \times \Delta z}$ , denoted below as  $v$ , each element of which has a mass of  $i, j, k$ th unit cell.

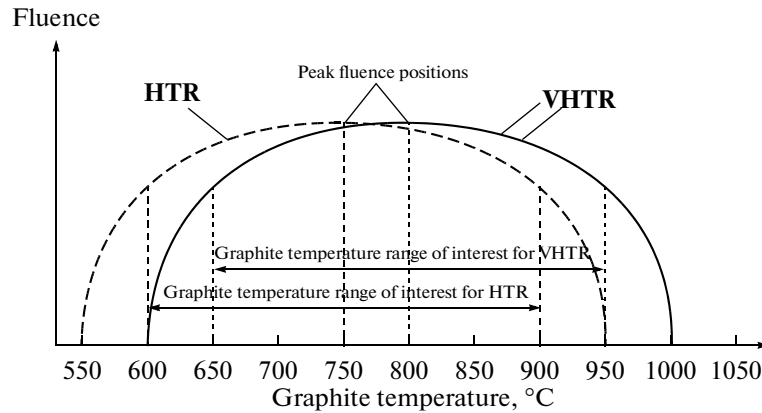


Fig. 2. Temperature range of operation of high-temperature gas-cooled reactors of Generations III (dashed line) and IV (solid line).

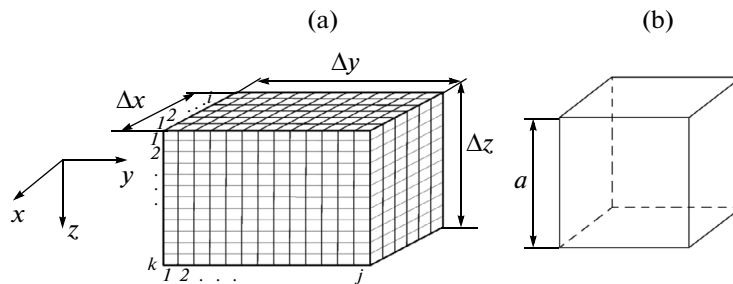


Fig. 3. Scheme of sample transformation to the three-dimensional matrix  $v$ : (a) sample; (b) unit cell  $i, j, k$ .

The graphite sample (the GMZ graphite is considered as the model material) consists of a filler and binder in a ratio of three to one [12]. The filler is coke granules having certain dimensions. The sizes of the GMZ graphite granules are listed in the table [12].

Based on the given data, it was offered to perform the stage-by-stage model formation of the graphite sample taking into account the granulometric composition.

A granule formation has been conducted using the statistical approach that is based on defining the law of distribution of unit cells along the  $x$ ,  $y$ , and  $z$  axes, which allows the required granule shape to be specified depending on the graphite type and microstructure features: size, shape, and percentage of filler granules in the sample.

Packing granules in the model volume of graphite sample by means of the complete enumeration of all

possible positions is extremely difficult. The complication of this task grows as the sample dimensions increase. To accomplish this task, an algorithm for arranging granules was proposed and implemented (specifying an arbitrary placement of granules with the possibility of overlapping each other), followed by the procedure of displacing the granules inside the sample volume step-by-step until the moment when there are no overlaps.

Results of the GMZ graphite sample simulation are presented in Figs. 4 and 5. Red indicates the material residing on the sample border; the material inside the sample is blue.

A real graphite sample has open and closed porosities. The model assumes that the total porosity of the sample is an open one (and it is offered to be specified by the unit cells in which the graphite mass is zero) and that the porosity distribution over the sample is of a stochastic nature [13]. Thus, the choice of a cell that is

Granulometric composition of filler for GMZ graphite [12]

Size, mm	$1.5 \pm 0.5$	$0.5 \pm 0.3$	$0.3 \pm 0.09$	<0.09
Content, %	26	13	14	47

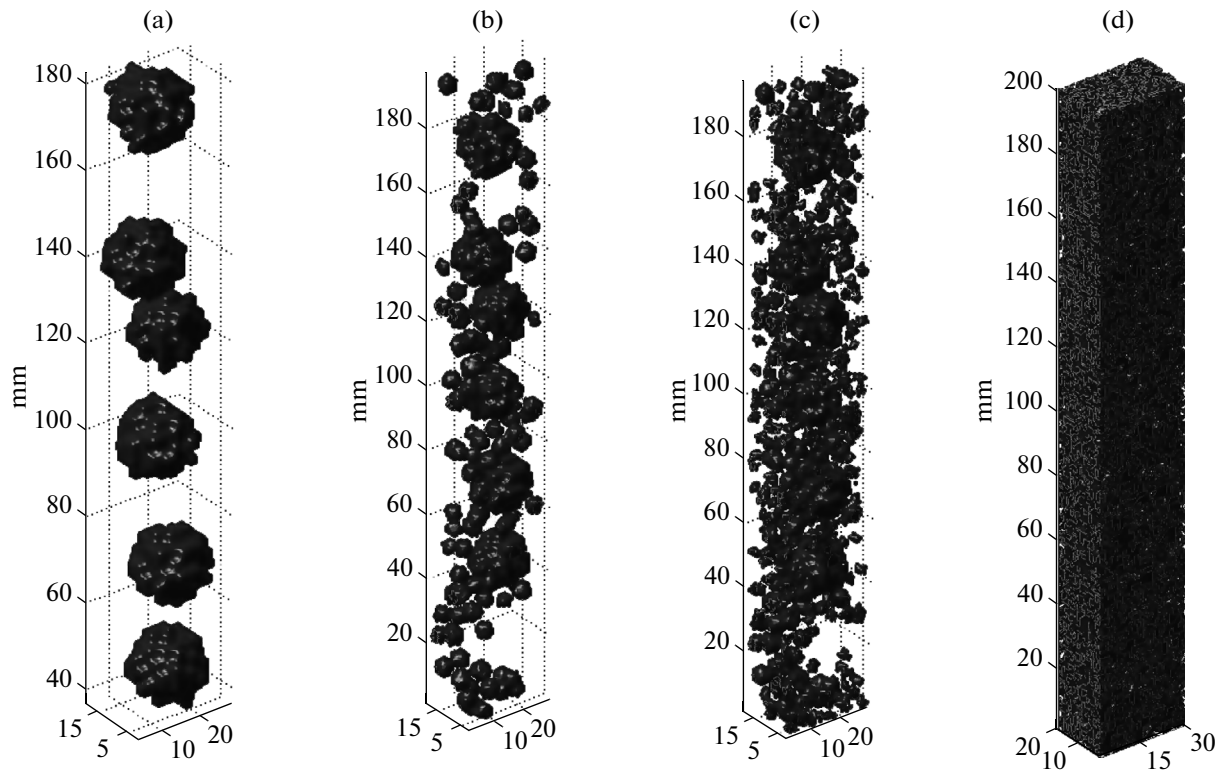


**Fig. 4.** Simulation of granulometric composition of the GMZ nuclear-grade graphite: (a) granules of a size of  $1.5 \pm 0.5$  mm, (b) addition of granules of  $0.5 \pm 0.3$  mm, (c) addition of granules of  $0.3 \pm 0.1$  mm, and (d) filler and binder.

a pore is implemented by means of a pseudorandom number generator (taking into account the porosity distribution over the sample filler and binder) based on the Mersenne Twister, which is devoid of many drawbacks inherent in the other generators such as a small period, predictability, and statistical dependence that is easily revealed [14–17].

The pores, whose dimensions are less than those of a unit cell, are not considered in the simulation model.

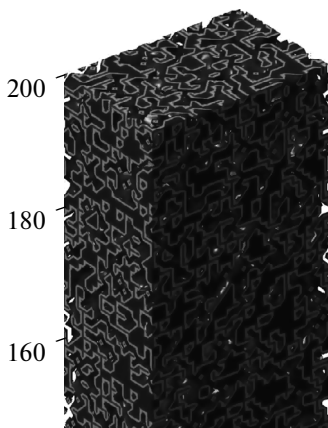


**Fig. 5.** Computer model of graphite: filler and binder (enlarged).

The mass of the sample unit cell is defined by the formula

$$m_{i,j,k} = a^3 \cdot \rho_{i,j,k}, \quad (2)$$

where  $a$  is the size of the unit-cell face,  $m$ ;  $\rho_{i,j,k}$  is the density of the  $i, j, k$ th unit cell,  $\text{kg}/\text{m}^3$ .

The sample mass is calculated by a formula without account for changes in linear dimensions of the sample:

$$M = \sum_{i=1, j=1, k=1}^{\frac{\Delta x}{a}, \frac{\Delta y}{a}, \frac{\Delta z}{a}} m_{i,j,k}, \quad (3)$$

$i = 1, 2, \dots, \Delta x$ ,  $j = 1, 2, \dots, \Delta y$ ,  $k = 1, 2, \dots, \Delta z$ ,

where  $m_{i,j,k}$  is the mass of the  $i, j, k$ th unit cell,  $\text{kg}$ ; a partition step is a multiple of all linear dimensions of the sample.

As has been mentioned above, Generation IV nuclear power systems are operated within a temperature range from 600 to 1000°C [11]; this simulation model considers a temperature range of 400 to 800°C, which corresponds to the diffusion regime described in [3, 18]. One peculiarity of this regime is the homogeneous oxidant distribution over the volume, since the reaction rate is less than a rate of the oxidant diffusion deep into the sample [8].

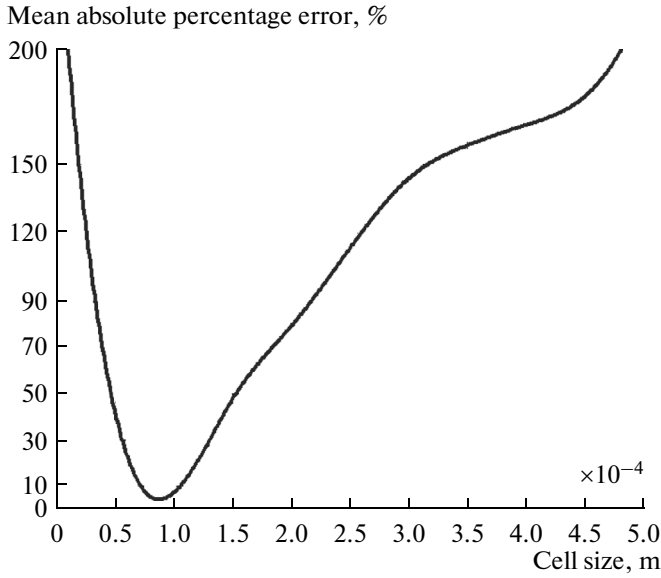


Fig. 6. Mean absolute percentage error of the simulation model of graphite oxidation.

A reduction in the mass of sample cell as a result of oxidation is calculated by the formula

$$\frac{dm_{i,j,k}}{dt} = (1 - \xi(m_{i,j,k})) \cdot K_g \times \sum_{h=-1, l=-1, \chi=-1}^{1, 1, 1} \xi(m_{i+h, j+l, k+\chi}), \quad (4)$$

where  $\xi(m) = \begin{cases} 0, & |m| > 0 \\ 1, & m = 0 \end{cases}$  is the delta function;  $K_g =$

$K(C_0)^n S$  is the oxidation rate, kg/s;  $K$  is the reaction constant, whose temperature dependence obeys the

Arrhenius equation,  $\text{kg}/(\text{m}^2 \text{ s})$  [12]:  $K = K_0 e^{-\frac{E}{RT}}$ ;  $K_0$  is the function of graphite properties that is characterized by the degree of material crystallinity and its porosity,  $\text{kg}/(\text{m}^2 \text{ s})$ ;  $E_a$  is the energy of activation of the surface, J;  $R$  is the gas constant,  $\text{m}^2 \text{ kg}/(\text{s}^2 \text{ K mol})$ ;  $T$  is the temperature, K;  $C_0$  is the oxidant concentration near the surface;  $n$  is the reaction order ( $n$  depends on many factors, including the oxidation regime and anisotropy, and takes on a value from 0.5 to 3) [24];  $S$  is the reaction surface (the area of a single unit cell  $S = a^2$ ),  $\text{m}^2$ ; and, when the matrix of cell masses  $v$  goes beyond the range (if index is zero or its value exceeds the matrix size in the appropriate dimension),  $m_{i,j,k}$  equals zero. The rate of the change in the sample mass is calculated by summing the mass changes over all cells of the sample:

$$\frac{dM}{dt} = \sum_{i=1, j=1, k=1}^{\frac{\Delta x}{a}, \frac{\Delta y}{a}, \frac{\Delta z}{a}} \frac{dm_{i,j,k}}{dt}.$$

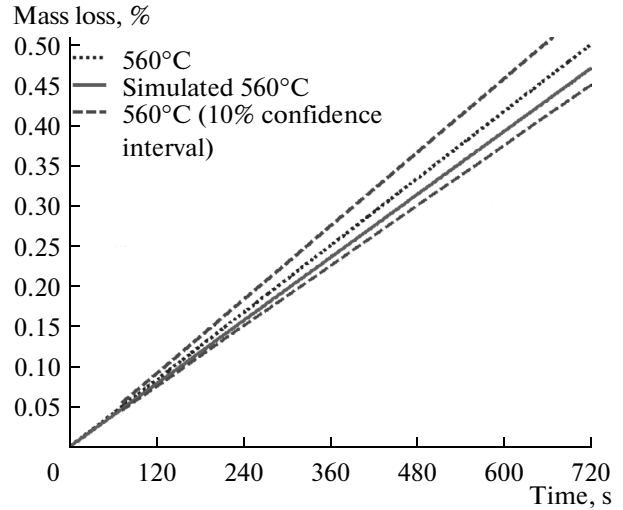


Fig. 7. Time dependence of mass loss of the graphite sample with a unit-cell size of 0.0001 m.

The simulation model is constructed on the basis of the assumption that internal pores of the sample contain an oxidant and oxidize inner cells at the same rate at which the external oxidant does. The cell density  $\rho_{i,j,k}$  and the cell mass  $m_{i,j,k}$  are specified from formulas (1) and (2), respectively.

For a determination of the model errors with respect to sizes of the unit cell, the numerical simulation of the graphite-sample oxidation was carried out at the temperature 560°C (Figs. 6, 7). The modeling-error calculation was performed using the mean absolute percentage error (MAPE) [22], which characterizes how large the modeling errors are in comparison with experimental data by the series values

$$\text{MAPE} = \frac{1}{n} \sum_{t=1}^n \frac{|Y_t - \widehat{Y}_t|}{Y_t} \times 100, \quad (5)$$

where  $n$  is the number of measurements,  $Y_t$  are the data of the experiment [24], and  $\widehat{Y}_t$  are the data of simulation.

An analysis of results obtained evidences that, while the unit-cell dimensions are reduced down to 0.0001 m, the error is around 7%; however, with a further decrease in size, an error growth is observed that is connected with the fact that the developed simulation model ignores the meso- and nanoscale phenomena, which begin to play a substantial role [20, 21] at sizes comparable with the molecule free path [23]. Thus, the field of application for the developed simulation model with an error of 7% is sample discretization comparable with 0.0001 m.

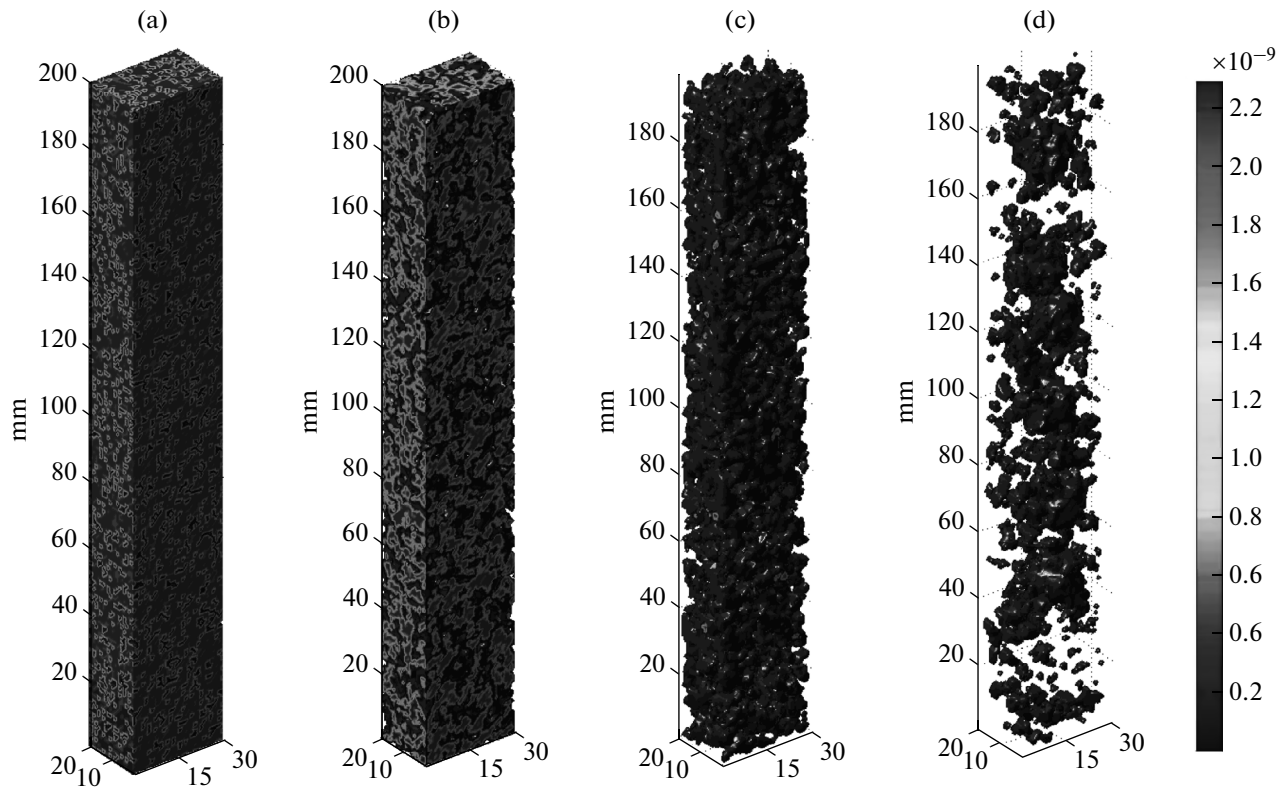


**Fig. 8.** View of the GMZ graphite sample during oxidation in an environment with a 10% concentration of oxidant  $O_2$  at a temperature of  $560^\circ C$ : initial state, (b) in 10 days, (c) in 20 days, and (d) in 30 days (scale of change in mass of a unit cell on the right).

## VERIFICATION OF SIMULATION MODEL

The simulation model was verified using the mathematical statistical apparatus [19] in the environment of Octave 3.6.4 mathematical package. The oxidation of a sample of the GMZ nuclear-grade graphite (as a model material) was simulated with the following characteristics: density  $1850 \text{ kg/m}^3$ ; porosity 20%; the granulometric composition given in the table [12]; linear dimensions of the sample amounting to 0.002 m in width, 0.003 m in length, and 0.02 m in height; and the 0.0001-m step of partitioning the sample into cubic unit cells with a given edge length. Parameters of the oxidation process were as follows: temperature  $560^\circ C$ ,  $O_2$  oxidant concentration 10%, oxidation rate  $K_g = 10^{-7} \text{ kg/s}$ , and process duration 30 days.

An analysis of simulation results (Fig. 8) shows the sample oxidation dynamics: a significant structural change is observed in 10 days; after 20 days the sample loses the properties of a load-bearing frame, while after 30 days a complete destruction of the sample is observed. Here it should be noted that a simulation with account for the sample porosity allowed the non-linearity and stochasticity of the graphite oxidation process to be taken into consideration. As can be seen from Fig. 8d, the account for oxidant penetration deep into the sample during the simulation substantially influences the destruction process, because the oxida-

tion occurs not only over external surfaces but also in the entire volume of the sample.

The simulation results obtained using the developed simulation model correlate well with experimental data presented in [24].

## CONCLUSIONS

Theoretical studies are performed and a simulation model of nuclear-grade graphite oxidation is developed that takes into account the porosity, fractional properties, diffusion of the oxidant, and the sample density for oxidation in the regime of chemical kinetics within the temperature range  $400\text{--}800^\circ C$ . The study results, verified in a simulation of the oxidation of GMZ nuclear-grade graphite at high temperature, satisfactorily agree with experimental data.

## REFERENCES

1. E. S. Kim and H. C. No, "Experimental study on the oxidation of nuclear graphite and development of an oxidation model," *J. Nucl. Mater.* **349** (1–2), 182–194 (2006).
2. A. Blanchard, "Appendix 2: The thermal oxidation of graphite," in *Irradiation Damage in Graphite due to Fast Neutrons in Fission and Fusion Systems: IAEA-TECDOC-1154* (IAEA, Vienna, 2000).

3. M. S. El-Genk and J.-M. P. Tournier, “Comparison of oxidation model predictions with gasification data of IG-110, IG-430 and NBG-25 nuclear graphite,” *J. Nucl. Mater.* **420** (1–3), 141–158 (2012).
4. H. Badenhorst, B. Rand, and W. W. Focke, “Modelling of natural graphite oxidation using thermal analysis techniques,” *J. Therm. Anal. Calorim.* **99** (1), 211–228 (2010).
5. W. S. Cornwall, *Wigner Stresses: TRG Report 40 (R)* (UKAEA, 1962).
6. M. Lasithiotakisa, B. J. Marsden, and T. J. Marrow, “Application of an independent parallel reactions model on the annealing kinetics of BEPO irradiated graphite,” *J. Nucl. Mater.* **427**, 95–109 (2012).
7. H. Li, S. L. Fok, and B. J. Marsden, “An analytical study on the irradiation-induced stresses in nuclear graphite moderator bricks,” *J. Nucl. Mater.* **372**, 164–170 (2008).
8. J. J. Lee, K. G. Tushar, and K. L. Sudarshan, “Oxidation rate of nuclear-grade graphite NBG-18 in the kinetic regime for VHTR air ingress accident scenarios,” *J. Nucl. Mater.* **438** (1–3), 77–87 (2013).
9. R. P. Wichner, T. D. Burchell, and C. I. Contescu, “Penetration depth and transient oxidation of graphite by oxygen and water vapor,” *J. Nucl. Mater.* **393** (3), 518–521 (2009).
10. H. Badenhorst and W. Focke, “Comparative analysis of graphite oxidation behaviour based on microstructure,” *J. Nucl. Mater.* **442**, 75–82 (2013).
11. M. Davies, “Qualification of selected graphites for a future HTR,” at *Technical Meeting on High-Temperature Qualification of High Temperature Gas-Cooled Reactor Materials* (IAEA, Vienna, 2014).
12. V. V. Goncharov, N. S. Burdakov, V. I. Karpukhin, and P. A. Platonov, *Effect of Irradiation on Graphite of Nuclear Reactors* (Atomizdat, Moscow, 1978).
13. V. S. Ostrovskii, I. N. Krutova, T. D. Shashkova, and A. P. Fedoseev, “Variations in Porosity and Penetrability of a Carbon Material during the Heat Treatment,” in *Structural Materials Based on Graphite (Collection of works no. 3)* (Metallurgiya, Moscow, 1967), pp. 204–208.
14. V. P. Kichor, R. V. Feshchur, V. V. Kozik, S. I. Vorobets, and N. E. Selyuchenko, *Economical and Statistical Modeling and Forecasting* (L’viv’ska Politekhnik National University Press, L’viv, 2007).
15. M. Matsumoto and T. Nishimura, “Mersenne Twister: a 623-dimensionally equidistributed uniform pseudo-random number generator,” *ACM Trans. Model. Comput. Simul.* **8** (1), 3–30 (1998).
16. SIMD-oriented Fast Mersenne Twister (SFMT): Twice Faster than Mersenne Twister. <http://www.math.sci.hiroshima-u.ac.jp/~m-mat/MT/SFMT/index.html>
17. R. Tor, Collusion-Secure Fingerprinting. A Simulation of the Boneh and Shaw Scheme. Coding Theory and Cryptography. Bergen: Department of Informatics Universitas Bergensis. [www.ii.uib.no/~georg/coding/Students/Tor/collusion\\_secure\\_fp.pdf](http://www.ii.uib.no/~georg/coding/Students/Tor/collusion_secure_fp.pdf)
18. H. Badenhorst, *Graphite Oxidation* (DST Chair in Carbon Materials and Technology, Pretoria, 2009).
19. A. M. Odeichuk and A. Yu. Gud, “Simulation model for studying heteroskedastic time series in information systems,” *Visnik Akademii Mitnoi Sluzhbi Ukraïni*, no. 1, 102–110 (2010).
20. N. F. Morozov, R. V. Gol’dshstein, and V. A. Gorodtsov, *Simulation of Mechanical Behavior of Nanostructural Formations* (St. Petersburg State University, Ishlinskii Institute for Problems in Mechanics, RAN, Moscow, 2009).
21. A. S. Lobasov and A. V. Minakov, “Computer simulation of heat and mass transfer processes in microchannels using the  $\sigma$ -Flow CFD-package,” *Komp. Issled. Modelir.* **4** (4), 781–792 (2012).
22. A. N. Odeichuk, “Generalized criterion of efficiency of models of predicting time series in information systems,” *Bionika Intelektu*, no. 1, 113–119 (2009).
23. *Processes of Micro- and Nanotechnology* (SPbGETU, St. Petersburg, 2010).
24. S. J. Gregg and R. F. S. Tyson, “The kinetics of oxidation of carbon and graphite by oxygen at 500°C–600°C,” *Carbon* **3** (1), 39–42 (1965).

*Translated by M. Samokhina*